



OPEN

# Water Amount Dependence on Morphologies and Properties of ZnO nanostructures in Double-solvent System

Jinzhou Yin<sup>1,2,3</sup>, Feng Gao<sup>1</sup>, Chengzhen Wei<sup>1,2</sup> & Qingyi Lu<sup>2</sup>

<sup>1</sup>Department of Materials Science and Engineering, Nanjing University, Nanjing 210093, P. R. China, <sup>2</sup>State Key Laboratory of Coordination Chemistry, Coordination Chemistry Institute, Nanjing National Laboratory of Microstructures, Nanjing University, Nanjing 210093, P. R. China, <sup>3</sup>School of Chemistry and Chemical Engineering, Huaiyin Normal University, Huai'an 223300, P. R. China.

Received  
29 July 2013

Accepted  
16 December 2013

Published  
17 January 2014

Correspondence and requests for materials should be addressed to F.G. (fgao@nju.edu.cn) or Q.Y.L. (qylu@nju.edu.cn)

ZnO materials with a range of different morphologies have been successfully synthesized via a simple double-solvothermal method in the presence of glycine. The morphologies of the products can be controlled from superstructures to microrods by adjusting the amount of water in the EtOH/H<sub>2</sub>O system. Photoluminescence (PL) studies reveal that the more amount of water was used, the stronger PL relative intensity of the green emission is, but the weaker ultraviolet emission. This might be attributed to the more defects of the products when the more water was used. The catalytic studies show that all the samples have good abilities to decrease decomposition temperature around 300°C and the decomposition temperature lowers with the increase of the relative intensity of ZnO green emission.

Control of the structure, size, and shape of inorganic materials has received increased attention in current materials syntheses due to the fact that they play very important roles in correlating to their magnetic, electrical, optical, and other properties<sup>1–4</sup>. Over the past two decades, a wide range of one-dimensional nanostructures, such as wires, rods, belts, and tubes, has been prepared<sup>5–8</sup>. So far, based on these 1D forms, intensive attention has been attracted to realization of 3D superstructures by patterning micro-/nano-structured building blocks with complex geometry, due to their unique properties for potential applications<sup>9,10</sup>. Commonly, surfactants are used as additives to assist the synthesis of materials with 3D superstructures. Therefore, developing facile, solution-based, morphology-controlled methods to fabricate novel self-assembled architectures remains challenge.

Zinc oxide (ZnO), an important semiconductor with a band gap of 3.37 eV at room temperature, has attracted great interests due to its unique properties and wide applications in field effect transistors, chemical sensors, transparent conductors, and ultraviolet light emitting devices<sup>11–14</sup>. The properties of ZnO are strongly dependent on its morphology and aspect ratio, as well as on the size, orientation, and density of the crystal<sup>15–17</sup>. And these structural characteristics have important applications in optoelectronics and photocatalysts. ZnO with different morphologies has been produced by various synthetic methods<sup>18</sup>. The solution based methods, such as solvothermal/hydrothermal and sol-gel processes, are attractive because the synthesis conditions used are mild and the processes are very simple. Compared to the conventional hydrothermal/solvothermal process, in which commonly only one kind of solvent is used, a double-solvothermal or a mixed-solvothermal process would have much greater influences on the structural control for various materials, because the properties of the mixed solvent can be controlled by adjusting the type and volume ratio of the solvents<sup>19</sup>.

In biomineralization, organisms can exert great control over mineral deposition from the solution phase by using biological molecules as matrices or molds<sup>20</sup>. The biomimetic syntheses of inorganic materials have been intensively researched to mimic the effects of soft biological molecules on the crystallization of inorganic materials<sup>21–23</sup>. Understanding the interactions between soft biomaterials and inorganic materials is very important to fabricating various materials with novel structures. Glycine is the simplest amino acid which is one of the fundamental components of biological molecules. It can form complexes with various metal ions, such as Fe<sup>2+</sup>, Cu<sup>2+</sup> and Zn<sup>2+</sup> in solution. Thus it is believed to have potentials as a kind of growth modifier in the synthesis of ZnO crystals. In this paper, we reported the synthesis of ZnO materials with various distinct morphologies by simple double-solvothermal (ethanol and water) method in the presence of glycine. By adjusting the ratio of ethanol and water, different morphologies of ZnO can be controllably synthesized. The optical properties and



catalytic efficacy were also explored and ZnO materials with different crystal growth habits show differences in these properties.

## Results

XRD was used to investigate the phase purity of the as-prepared ZnO, as shown in Figure 1a. All the diffraction peaks can be indexed to the hexagonal wurtzite-structure of ZnO (JCPDS 36-1451) and the sharpness of the peaks implies the high crystalline quality of the as-prepared sample. No peaks of impurities can be detected, demonstrating that ZnO with high purity has been synthesized successfully by the solution phase approach using a double solvent system consisting of water and ethanol in the presence of glycine. Figure 1b–d shows typical SEM images of ZnO samples prepared through the typical procedure. An SEM image with a low magnification (Figure 1b) displays that the sample is composed of microspheres. An SEM image with high magnification (Figure 1c) on side view reveals that the ZnO microspheres are mushroom-like superstructures. The top view of the sample (Figure 1d) shows that the superstructure is made up of numerous of hexagonal disks. The diameter of the hexagonal disks is in the range of 100–150 nm, and the

thickness is about 50 nm. The numerous disks are assembled to form the mushroom-like structure. This complex morphology can be obtained on a large scale. Figure 1e shows a typical TEM image of ZnO microspheres while Figure 1f shows a fragment disk of the ZnO microspheres. The inserted selected area electron diffraction (SAED) pattern in Figure 1f confirms the single-crystalline nature of the disk.

The double-solvent reaction system was studied by monitoring the influence of water volume with a constant amount of zinc acetate and glycine on the morphology of products by microscopy investigations. Figure 2 shows SEM images of the prepared products with different amount of water. Without the addition of water (0 ml), the obtained product is composed of spheres as SEM shows in Figure 2a–b when zinc acetate and glycine was treated under ethanol-thermal conditions. The spheres are assembled by nanoparticles with size of about 20 nm. It can be also observed that the spheres are hollow inside as the broken spheres in the SEM images confirm. Increasing the used water volume to 2.0 ml, a complex superstructure assembled by hexagonal disks was obtained as shown in Figure 2c–d. Interestingly, the superstructure has a hexagonal hoop in the middle like a waistband. As the water amount was further increased to

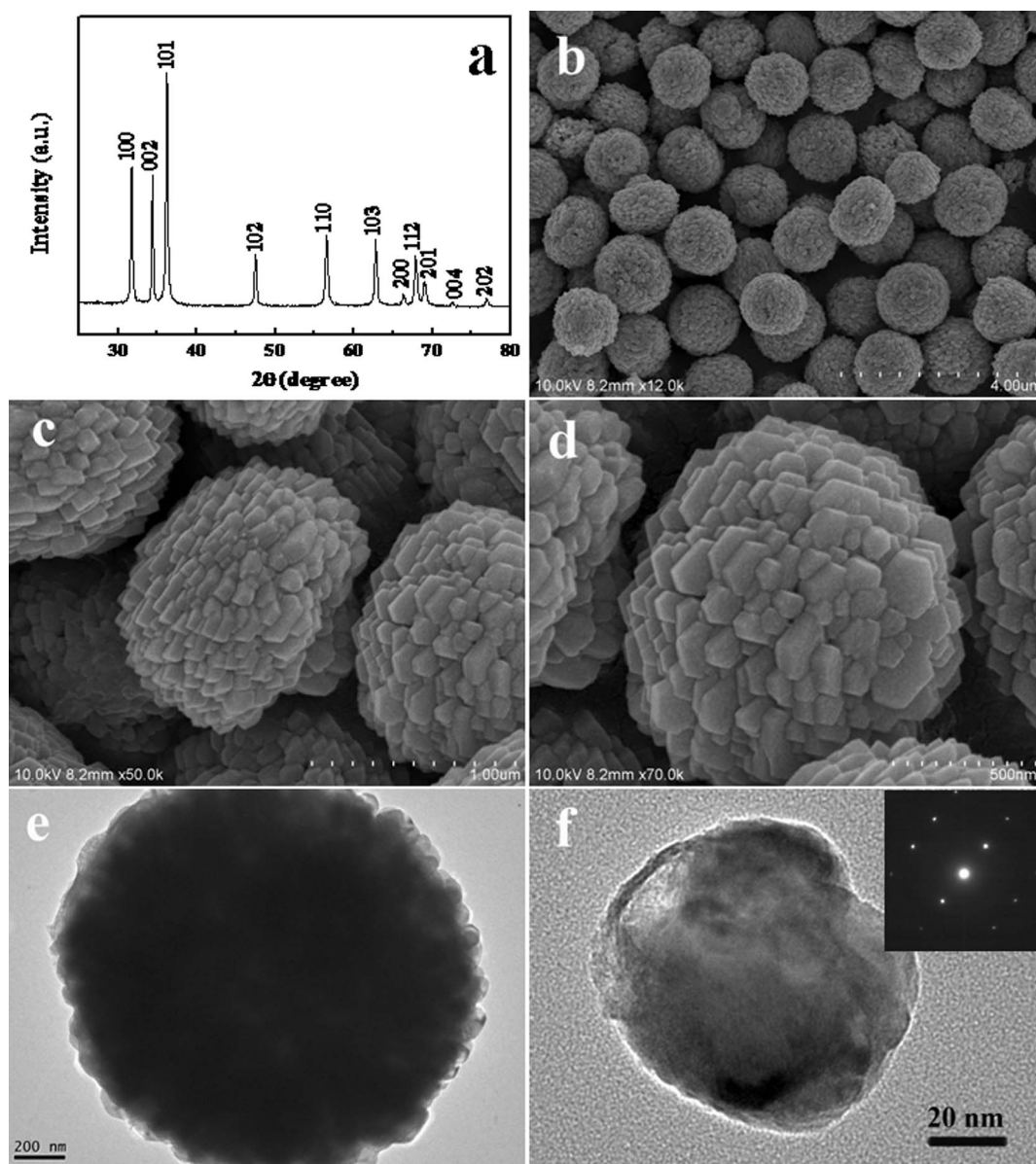


**Figure 1** | (a) XRD pattern, (b ~ d) SEM images, (e) TEM image of the as-prepared sample, (f) TEM image of a fragment of the ZnO microspheres (the inset part: corresponding SAED pattern).

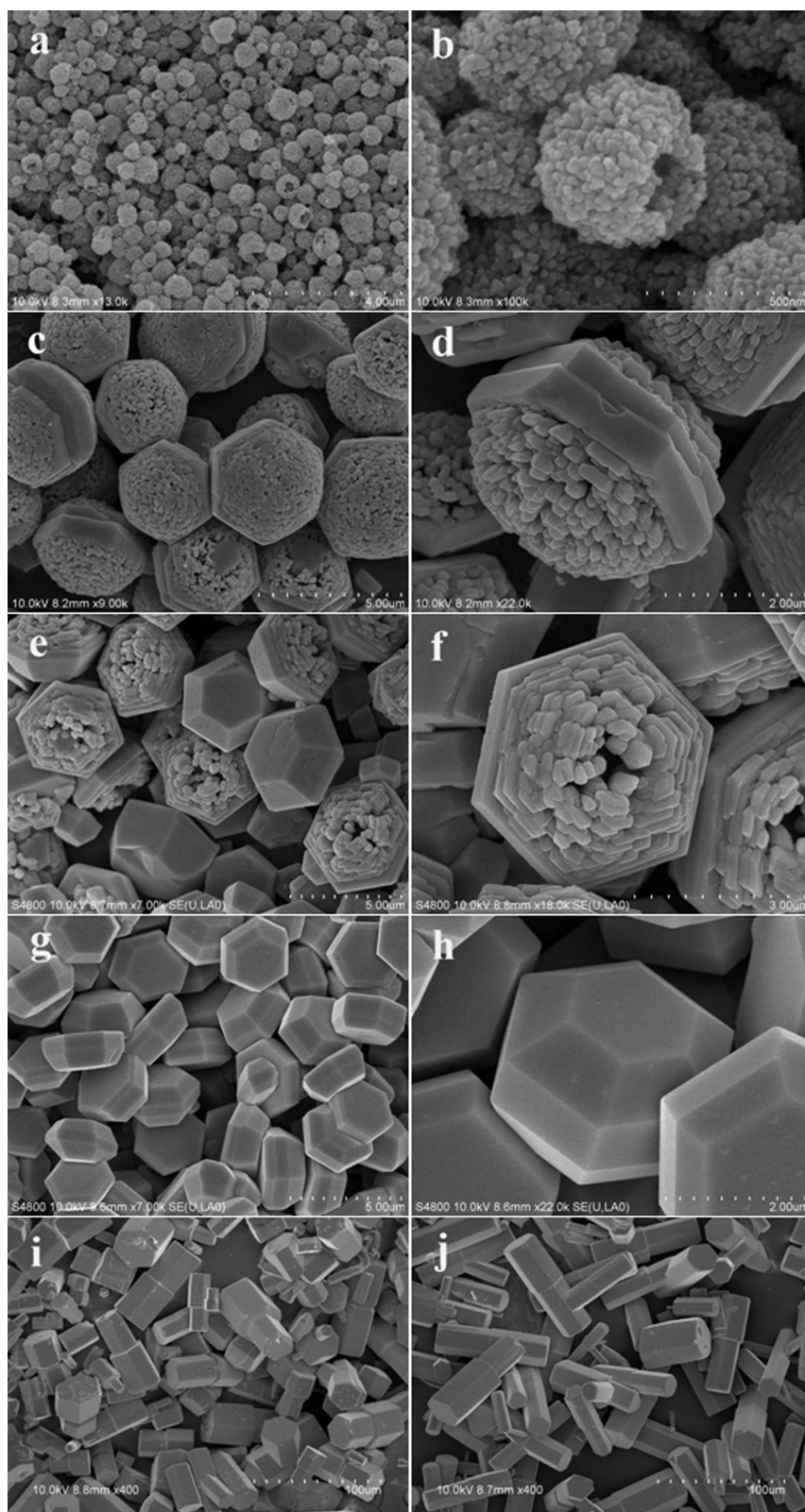


**Figure 2** | SEM images of the samples prepared with different amount of water: (a, b) 0 mL; (c, d) 2.0 mL; (e, f) 4.0 mL; (g, h) 5.0 mL, (i) 7.0 mL and (j) 8.0 mL.

4.0 ml, SEM images (Figure 2e–f) display that the obtained sample has a “potted plant”-like structure. On one side, the sample has a perfect polyhedral morphology like a “pot”, while from the other side, it can be observed that the part in the middle of the superstructures are composed of hexagonal disks. The thickness of the

disk is about 300 nm. When the water volume is increased to 5.0 mL (Figure 2g–h), polyhedral microdisks with different facets exposed are obtained. These polyhedral microdisks are like two “pot” in Figure 2e to connect to each other. When the amount of water is further increased to 7.0 mL or 8.0 mL, only ZnO microrods

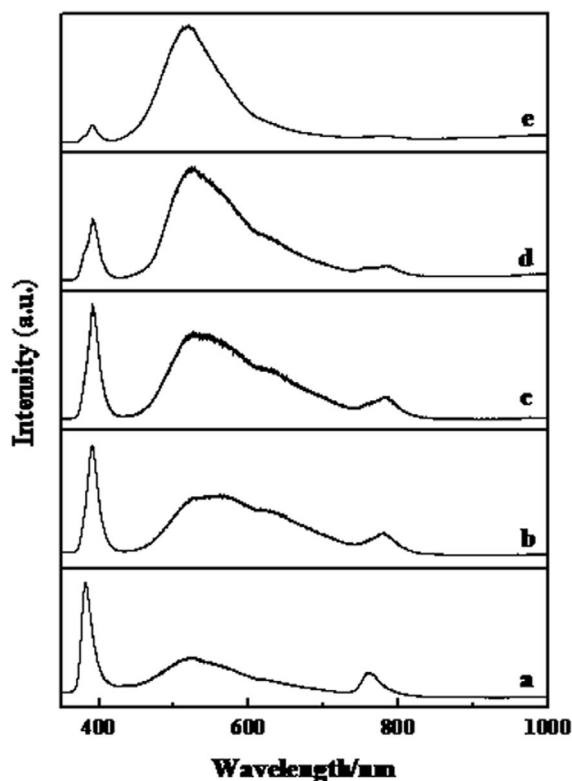


**Figure 3** | Room-temperature photoluminescence spectra of the samples prepared with different amount of water: (a) 0 mL; (b) 0.5 mL; (c) 2.0 mL; (d) 4.0 mL; and (e) 5.0 mL.

can be obtained as shown in Figure 2i and j. From Figure 1b–c and Figure 2, when the volume of water increased from 0 mL to 8.0 mL, the morphology of the obtained ZnO changed from the superstructure of nanoparticles and disks, pure disks to rods.

## Discussion

SEM observations of the products reveal that the amount of added water in the double-solvent system is the key factor to control the morphology evolution of the obtained ZnO crystals. The microstructure and the size of the as-prepared ZnO particles depend closely on the amount of water added. As the amount of water increases, the morphology of the obtained ZnO changes from the superstructure assembled by nanoparticles and disks, pure disks to rods. It is very interesting to note that the structure and size of ZnO particles can be controlled only by adjusting the amount of water in the ethanol solution. Therefore it is important to understand the formation of ZnO particles. In this study, the zinc acetate dihydrate was used as zinc source, and reaction conditions, such as reaction temperature and reaction time, were kept the same for all of the reactions. Therefore, the obtained ZnO particles with different morphology and size can only due to the effects of the solvents with different amount water. The polarity, viscosity and solvency of the solvents change with the addition of different amount of water. Solvents with different polarity, viscosity and solvency may cause different crystal growth habits. The polarity of solvents influences not only the nucleation of the ZnO crystals but also the preferential direction of the crystal growth<sup>24</sup>. In solvents with high polarities, the growth along the [001] direction was enhanced, which resulted in rodlike morphologies. As the amount of water increases, the polarity of the solvents enhances accordingly. On the other hand, the solubility of ZnAc<sub>2</sub> and glycine was different in the ethanol solution with different amount of water. The molecule of zinc acetate and glycine is hardly soluble in ethanol and soluble in water. In the absence of

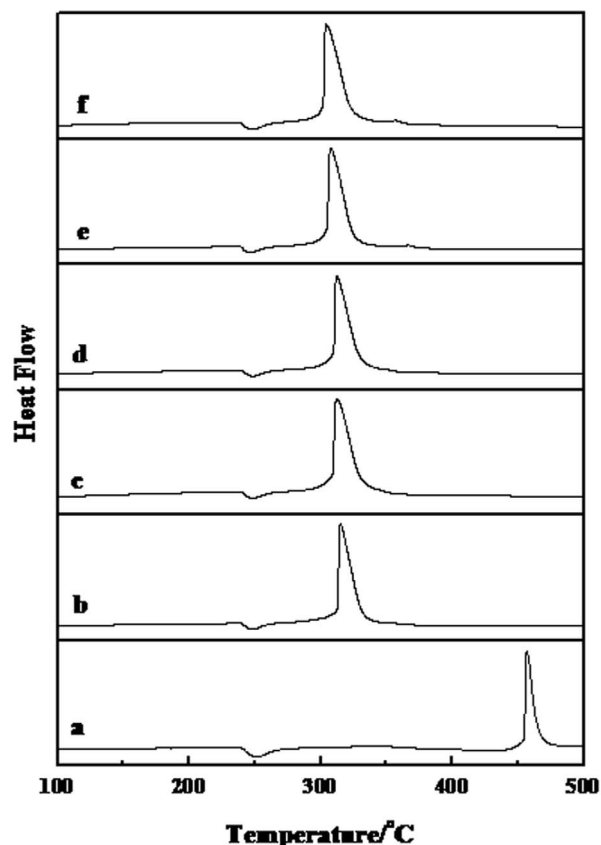


**Figure 4** | DSC curves of pure AP (a) and the mixture of AP with the ZnO structures obtained with 1.0 mmol of glycine and different amount of H<sub>2</sub>O: (b) 0 mL; (c) 0.5 mL; (d) 2.0 mL; (e) 4.0 mL and (f) 5.0 mL.

water, zinc acetate and glycine can not dissolve in anhydrous ethanol. As the amount of water increases, more and more of the molecule of ZnAc<sub>2</sub> and glycine dissolve in the ethanol and water solution, which might lead to the fast growth of ZnO crystal and result in the formation of polyhedral ZnO microdisks and ZnO microrods with perfect morphology. In the reaction system, the presence of glycine is also of great importance. The molecule of glycine contains an amino group and a carboxylic acid group. Without the addition of glycine, the products would display different morphology from those presented in this study. With the increase of water, more and more of zinc acetate and glycine dissolve in the water and the zinc ions might coordinate with glycine molecules to form complex intermediates. The space hindrance of the zinc glycine complex would affect the growth ZnO crystals. So the morphology of the ZnO can be successfully controlled by adjusting the amount of water in the reaction system.

Room-temperature photoluminescence (PL) properties of the obtained ZnO superstructures prepared with different amount of water at an excitation wavelength of 325 nm were studied. As shown in Figure 3, an ultraviolet (UV) emission around 390 nm and a green band at 530 nm can be observed for all the ZnO samples. The UV emission corresponds to the near band edge emission of wide band gap of ZnO due to the recombination of excitonic centers. The green band emission is associated with the intrinsic defect centers like oxygen vacancy, zinc vacancy, zinc interstitial, oxygen interstitial, or antisite oxygen<sup>25–28</sup>. From Figure 3, it can be also observed that with the more amount of water used, the PL relative intensity of the green emission becomes stronger, but the ultraviolet emission weaker. That might be attributed to the more defects of the products when the more water was used in the double-solvent system. As the amount of water increases, more and more of the molecule of glycine

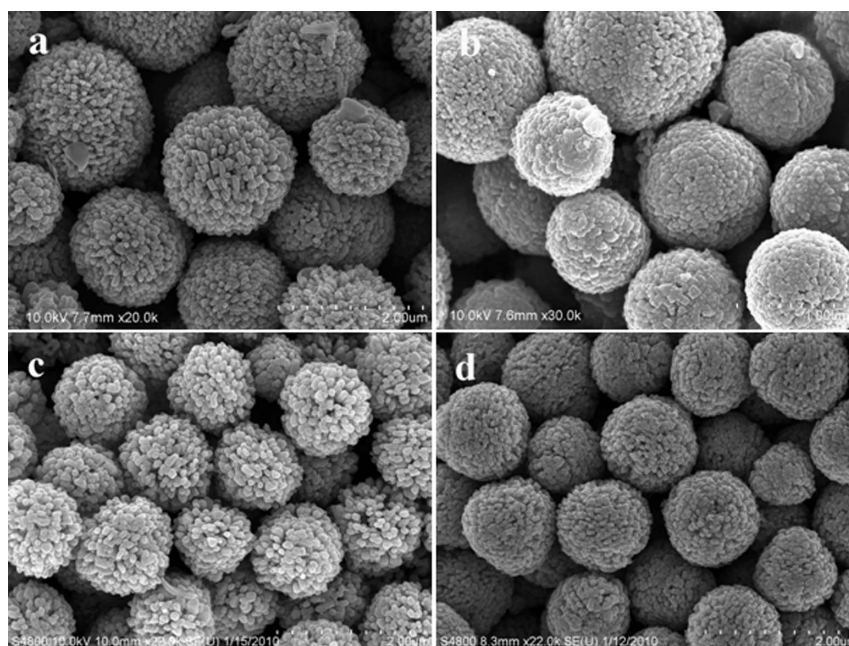


**Figure 5** | SEM image of the ZnO samples prepared under different conditions with the addition of 0.5 ml water: (a) 180 °C, 12 h; (b) 220 °C, 12 h; (c) 200 °C, 6 h and (d) 200 °C, 24 h.

dissolve in the solvent. The molecule of glycine contains an amino group and a carboxylic acid group and can trap zinc ions to form zinc glycine complex. This kind of reaction may cause zinc vacancy on the surface of ZnO particles. As the amount of water increases in the reaction system, there are more zinc vacancies on the surface of ZnO crystals, leading to the relatively stronger green emission in PL spectra.

The catalytic properties for decomposition of ammonium perchlorate (AP) of the different ZnO structures were also studied. Figure 4 shows the DSC curves of both pure AP and the mixtures

of AP with the ZnO structures obtained with 1.0 mmol of glycine and different amount of H<sub>2</sub>O at a 2% mass basis. From Figure 4a, the first endothermic peak at 245 °C is due to the crystal transformation of AP from orthorhombic to cubic phase and the exothermic peak around 450 °C corresponds to the thermal decomposition of AP<sup>29,30</sup>. From the DSC curves of the mixtures of AP and ZnO samples (Figure 4b–4f), the exothermic peaks corresponding to the thermal decomposition of AP occurred at temperatures around 300 °C. Compared with the thermal decomposition of pure AP, the AP decomposition was accelerated dramatically in the presence of ZnO samples. The

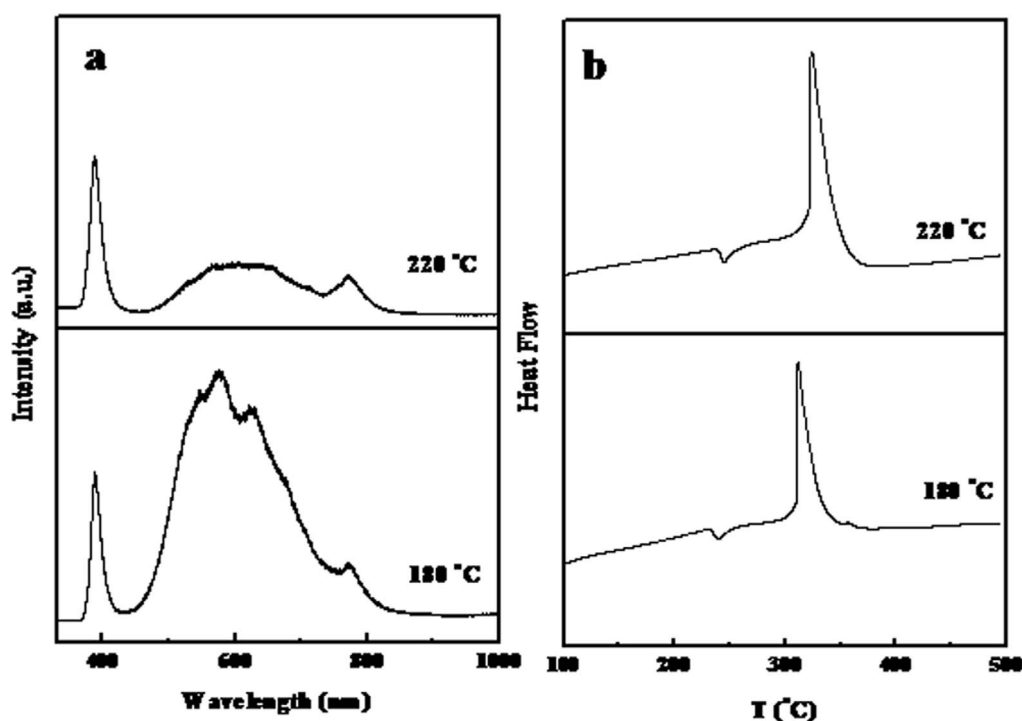


**Figure 6** | (a) Room-temperature photoluminescence spectra of the samples prepared at different temperatures and (b) DSC curves of the mixture of AP with the ZnO structures obtained at different temperatures.

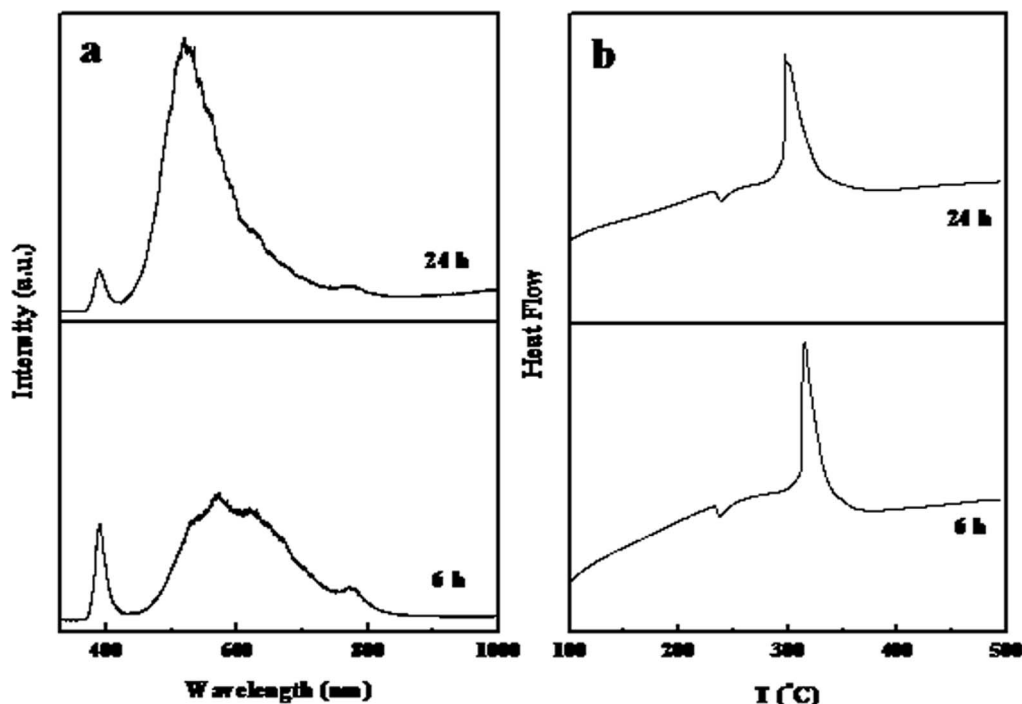


**Figure 7** | (a) Room-temperature photoluminescence spectra of the samples prepared for different time and (b) DSC curves of the mixture of AP with the ZnO structures obtained for different time.

decomposition temperatures of AP with the ZnO samples prepared with different amount of H<sub>2</sub>O are about 315°C, 310°C, 311°C, 308°C and 302°C, respectively. The ZnO catalytic properties of AP decomposition should be related to their structures. The more amount of water was used; the more defects on the surface of ZnO from PL spectra, and the lower temperature for AP decomposition. The defects on the surface might be helpful on the ZnO catalytic properties of AP decomposition.

Besides the added water amount, the effects of other experimental conditions, such as reaction temperature and reaction time, on crystal growth and thus intrinsic defects were also studied. Figure 5a and b show SEM images of the samples prepared with the addition of 0.5 ml water at different temperatures. The obtained ZnO samples are composed of nanoparticle-assembled spheres. As the reaction temperature increases, the assembled units grow bigger and become more regular. Figure 6a shows the room temperature photoluminescence spectra of the samples prepared at different temperatures. As the reaction temperature increases, the PL relative intensity of the green emission becomes weaker. With the same amount of water, the ZnO crystals become more regular with the reaction temperature increasing and the more regular ZnO crystals may results in less defects, leading to weaker green emission. Accordingly, with the defects on surface changing, the catalytic properties for AP decomposition change. Figure 6b shows the DSC curves of the mixture of AP with the ZnO structures obtained at different temperatures. The decomposition temperatures of AP with the ZnO samples prepared at 180 and 200°C are about 310°C and 324°C, respectively, demonstrating that the defects on the surface might be helpful for the ZnO catalytic properties of AP decomposition and more defects would lower the decomposition temperature of AP. On the other hand, the reaction time also show same variation tendency of PL and catalytic properties. Figure 5c and d show SEM images of the samples prepared with different time when the added water amount is 0.5 ml. The ZnO particles were composed of ZnO disks and the ZnO disks pack closer as the reaction time increases. From PL spectra of the samples prepared with different time as shown in Figure 7a, it can be observed that as the reaction time increases the PL relative

intensity of the green emission becomes stronger, indicating the more defect on the ZnO surface. This result should be relative to the fact that with the increase of reaction time, the remaining glycine in the reaction system would react with Zn atoms on the surface of ZnO crystals to form more defects. The more defects on the surface lower the AP decomposition temperature, which can be observed from DSC curves in Figure 7b of the mixture of AP with the ZnO structures obtained with different time. Although up to now, the thermal decomposition mechanism of AP has not yet been fully understood because the decomposition process is a complex hetero-phase process involving coupled reactions in the solid, adsorbed and gaseous phases. According to the traditional electron-transfer theory<sup>31</sup>, the presence of partially filled 3D orbit in Zn<sup>2+</sup> provides help in an electro-transfer process. Our results show that ZnO crystals displaying stronger green emission would catalyze AP to thermally decompose at lower temperature. The green emission of ZnO crystals is reported to be contributed to zinc vacancy on the surface and the results demonstrate that the defects on the surface might be helpful on the electro-transfer to lower the AP decomposition temperature.

In summary, we proposed a double-solvent thermal method to controllably synthesize a series of ZnO samples in the presence of glycine. By adjusting the water amount in the EtOH/H<sub>2</sub>O system, the morphology of the products can be easily controlled from nanoparticles to microrods. The PL relative intensity of the green emission and the ultraviolet emission can be tuned by the amount of water. It is an effective way to control the optical properties by adjusting the experimental conditions. The catalytic studies show that all the samples have good abilities to decrease decomposition temperature of AP to around 300°C and the decomposition temperatures lower as the intensities of the green emission increase.

## Methods

**Synthesis.** All the reagents were analytical grade and used without further purification. In a typical synthesis, 0.5 mmol ZnAc<sub>2</sub>·2H<sub>2</sub>O and 1.0 mmol glycine were added into a solution of 20 mL ethanol and 0.5 mL deionized water with vigorous stirring. Then the reaction mixture was transferred into a 35 mL Teflon-lined autoclave and kept at 200°C for 12 h. When the reaction was complete, the



autoclave was allowed to cool to room temperature. The precipitate was collected and washed alternately with deionized water and ethanol several times, and dried in air at ambient condition.

**Characterizations.** Powder X-ray diffraction (XRD) measurements were performed with an X-ray diffractometer (ULTIMA-3) at Cu K<sub>α</sub> radiation with 40 kV beam voltage and 40 mA beam current. The data were collected in the 20–80° range (2θ) with steps of 0.02. Scanning electron microscopy (SEM) images were obtained with a Hitachi S-4800 field-emission microscope. Transmission electron microscopy (TEM), high-resolution TEM (HRTEM) images and selected area electron diffraction (SAED) patterns were obtained with a JEOL JEM-2100 transmission electron microscope with an acceleration voltage of 200 KV. The photoluminescence (PL) spectra were recorded on a LabRam HR 800 spectrometer (Jobin-Yvon) excited with a 30 mW xenon lamp (325 nm) at room temperature. The catalytic roles of ZnO in the thermal decomposition of AP were studied by differential scanning calorimeter (DSC) using STA 449C thermal analyzer at a heating rate of 20°C·min<sup>-1</sup> in N<sub>2</sub> atmosphere over the temperature range of 20–500°C. The mass percentage of ZnO to AP in the mixture is fixed at 2%.

- Wang, X., Zhuang, J., Peng, Q. & Li, Y. D. A general strategy for nanocrystal synthesis. *Nature* **437**, 121–124 (2005).
- Wang, X. D., Gao, P. X., Li, J., Summers, C. J. & Wang, Z. L. Rectangular porous ZnO-ZnS nanocables and ZnS nanotubes. *Adv. Mater.* **14**, 1732–1735 (2002).
- Yin, Y. D. & Alivisatos, A. P. Colloidal nanocrystal synthesis and the organic-inorganic interface. *Nature* **437**, 664–670 (2005).
- Xu, L. P. *et al.* ZnO with different morphologies synthesized by solvothermal methods for enhanced photocatalytic activity. *Chem. Mater.* **21**, 2875–2885 (2009).
- Goldberger, J., Sirbully, D. J., Law, M. & Yang, P. D. ZnO nanowire transistors. *J. Phys. Chem. B* **109**, 9–14 (2005).
- Hullavarad, S. S., Hullavarad, N. V., Karulkar, P. C., Luykx, A. & Valdivia, P. Ultra violet sensors based on nanostructured ZnO spheres in network of nanowires: a novel approach. *Nanoscale Res. Lett.* **2**, 161–167 (2007).
- Wang, X. D., Liu, J., Song, J. H. & Wang, Z. L. Integrated nanogenerators in biofluid. *Nano Lett.* **7**, 2475–2479 (2007).
- Zhang, B. P. *et al.* Formation of highly aligned ZnO tubes on sapphire (0001) substrates. *Appl. Phys. Lett.* **84**, 4098–4100 (2004).
- Gu, Z. J. *et al.* Controllable assembly of WO<sub>3</sub> nanorods/nanowires into hierarchical nanostructures. *J. Phys. Chem. B* **110**, 23829–23836 (2006).
- Lu, F., Cai, W. P. & Zhang, Y. G. ZnO hierarchical micro/nanoarchitectures: Solvothermal synthesis and structurally enhanced photocatalytic performance. *Adv. Funct. Mater.* **18**, 1047–1056 (2008).
- Arnold, M. S., Avouris, P., Pan, Z. W. & Wang, Z. L. Field-effect transistors based on single semiconducting oxide nanobelts. *J. Phys. Chem. B* **107**, 659–663 (2003).
- Rao, G. S. T. & Rao, D. T. Gas sensitivity of ZnO based thick film sensor to NH<sub>3</sub> at room temperature. *Sens. Actuat. B* **55**, 166–169 (1999).
- Huang, M. H. *et al.* Room-temperature ultraviolet nanowire nanolasers. *Science* **292**, 1897–1899 (2001).
- Tominaga, K. *et al.* Transparent conductive ZnO film preparation by alternating sputtering of ZnO:Al and Zn or Al targets. *Thin Solid Films* **334**, 35–39 (1998).
- Zhang, J. *et al.* Control of ZnO morphology via a simple solution route. *Chem. Mater.* **14**, 4172–4177 (2002).
- Jang, E. S., Won, J., Hwang, S. & Choy, J. Fine tuning of the face orientation of ZnO crystals to optimize their photocatalytic activity. *Adv. Mater.* **18**, 3309–3312 (2006).
- Zhao, Q. *et al.* Morphological effects on the field emission of ZnO nanorod arrays. *Appl. Phys. Lett.* **86**, 203115 (2005).
- Wang, Z. L. Zinc oxide nanostructures: growth, properties and applications. *J. Phys.: Condens. Matter* **16**, R829–R858 (2004).
- Pang, H., Gao, F. & Lu, Q. Y. Glycine-assisted double-solvothermal approach for various cuprous oxide structures with good catalytic activities. *CrystEngComm* **12**, 406–412 (2010).
- Zhan, J. H., Lin, H. P. & Mou, C. Y. Biomimetic formation of porous single-crystalline CaCO<sub>3</sub> via nanocrystal aggregation. *Adv. Mater.* **15**, 621–623 (2003).
- DiMasi, E., Kwak, S. Y., Pichon, B. P. & Sommerdijk, N. Structural adaptability in an organic template for CaCO<sub>3</sub> mineralization. *CrystEngComm* **9**, 1192–1204 (2007).
- Tseng, Y., Lin, H., Liu, M., Chen, Y. & Mou, C. Biomimetic synthesis of nacrelite faceted mesocrystals of ZnO-gelatin composite. *J. Phys. Chem. C* **113**, 18053–18061 (2009).
- Zolotoyabko, E. & Pokroy, B. Biomineralization of calcium carbonate: structural aspects. *CrystEngComm* **9**, 1156–1161 (2007).
- Ayudhya, S. K. N., Tonto, P., Mekasuwandumrong, O., Pavarajarn, V. & Praserthdam, P. Solvothermal synthesis of ZnO with various aspect ratios using organic solvents. *Cryst. Growth Des.* **6**, 2446–2450 (2006).
- Guo, L. *et al.* Synthesis and characterization of poly(vinylpyrrolidone)-modified zinc oxide nanoparticles. *Chem. Mater.* **12**, 2268–2274 (2000).
- Klason, P. *et al.* Temperature dependence and decay times of zinc and oxygen vacancy related photoluminescence bands in zinc oxide. *Solid State Commun.* **145**, 321–326 (2008).
- Manzano, C. V., Alegre, D., Caballero-Calero, O., Alén, B. & Martín-González, M. S. Synthesis and luminescence properties of electrodeposited ZnO films. *J. Appl. Phys.* **110**, 043538 (2011).
- Pandey, S. K. *et al.* Effect of growth temperature on structural, electrical and optical properties of dual ion beam sputtered ZnO thin films. *J. Mater. Sci. Mater. Electron.* **24**, 2541–2547 (2013).
- Yin, J. Z. *et al.* Hierarchical ZnO nanorod-assembled hollow superstructures for catalytic and photoluminescence applications. *Cryst. Growth Des.* **10**, 40–43 (2010).
- Sun, X. F., Qiu, X. Q., Li, L. P. & Li, G. S. ZnO twin-cones: Synthesis, photoluminescence, and catalytic decomposition of ammonium perchlorate. *Inorg. Chem.* **47**, 4146–4152 (2008).
- Said, A. A. & Al-Qasbi, R. The role of copper cobaltite spinel, Cu<sub>x</sub>Co<sub>3-x</sub>O<sub>4</sub> during the thermal decomposition of ammonium perchlorate. *Thermochim. Acta* **275**, 83–91 (1996).

## Acknowledgments

This work is supported by the National Natural Science Foundation of China (Grant No. 21071076 and 21201072), the Natural Science Foundation of Jiangsu Province (Grant Nos. BK2012241), China Postdoctoral Science Foundation (Grant No. 2013T60517 and 2012M511241), and Natural Science Foundation of Jiangsu Higher Education Institutions of China (Grant No.12JB150006).

## Author contributions

F.G. and Q.L. guided the entire project, carried out data analyses and co-wrote the manuscript. Y.J. and C.W. performed the experiments, characterizations and property tests. All the co-authors discussed the results and commented on the manuscript.

## Additional information

**Competing financial interests:** The authors declare no competing financial interests.

**How to cite this article:** Yin, J.Z., Gao, F., Wei, C.Z. & Lu, Q.Y. Water Amount Dependence on Morphologies and Properties of ZnO nanostructures in Double-solvent System. *Sci. Rep.* **4**, 3736; DOI:10.1038/srep03736 (2014).



This work is licensed under a Creative Commons Attribution-NonCommercial-ShareAlike 3.0 Unported license. To view a copy of this license, visit <http://creativecommons.org/licenses/by-nc-sa/3.0>